

# Near-wall cycle amplitude modulation in turbulent boundary layers

**Romain Mathis**

Department of Mechanical Engineering,  
University of Melbourne, Victoria 3010, Australia  
rmathis@unimelb.edu.au

**Nicholas Hutchins**

Department of Mechanical Engineering,  
University of Melbourne, Victoria 3010, Australia  
nhu@unimelb.edu.au

**Ivan Marusic**

Department of Mechanical Engineering,  
University of Melbourne, Victoria 3010, Australia  
imarusic@unimelb.edu.au

## ABSTRACT

A non-linear influence of the large-scale log-region motions onto the small-scale near-wall cycle is found to exist in the buffer and log-region of turbulent boundary layers. Based on recent observations of Hutchins & Marusic (2007b) in high Reynolds number turbulent boundary layers, a novel procedure is developed to evaluate the modulation effect. This is done using tools based on Hilbert transformations applied to the spectrally filtered small-scale component of fluctuating velocity signals. The procedure allows us to quantify the modulation level of small-scale motions imparted by the superstructure type-events. Further analysis shows a high degree of robustness for this method.

## INTRODUCTION

In wall-bounded turbulent flows, it is believed that the relationship between different scale motions could play an important role in the turbulence organisation. Despite numerous studies devoted to the understanding of such flows, there are still few solid observations of the organisation of large- and small-scale structures. The DNS (direct numerical simulation) study of Jiménez & Pinelli (1999) supported the view that the near-wall cycle of streaks and quasi streamwise vortices is self-sustaining and unaffected by the outer region, i.e. it is capable of regenerating even in the absence of external triggers or influences (Panton, 2001). However, this autonomous view was based largely on results from low Reynolds number studies ( $Re_\tau < 1000$ , where  $Re_\tau = \delta U_\tau / \nu$ , with  $\delta$  the boundary layer thickness,  $U_\tau$  the friction velocity and  $\nu$  the kinematic viscosity), which means by definition that the range of scales of motions and the scale separation are severely limited. More recently, advances in Particle Image Velocimetry and higher Reynolds number facilities have given further understanding of large scale structures, which exhibit clear Reynolds number dependencies (Adrian *et al.*, 2000; Ganapathisubramani *et al.*, 2003; Hutchins *et al.*, 2005). Newer DNS studies by del Álamo *et al.* (2004) and Hoyas & Jiménez (2008) have also reinforced this view. Experimental studies of Hutchins & Marusic (2007a) at higher Reynolds number ( $Re_\tau \sim 7000$ ), have revealed the presence of elongated regions ( $\sim 20\delta$ ) of

momentum deficit in the log-layer, called “superstructures” by the authors. These structures appear to be similar to the Very Large Scale Motions (VLSMs) described by Kim & Adrian (1999) and Adrian *et al.* (2000). The discovery of such very large-scale motions has in turn raised questions concerning their effect on the near-wall cycle. By studying fluctuating velocity signals from hot-wire sensors in the near-wall region, Hutchins & Marusic (2007b) recently observed that, in addition to the low-wavenumber mean shift, the largest scales appeared to be “amplitude modulating” the small-scale fluctuations. For the present paper, we expand upon the initial observations of Hutchins & Marusic (2007b) ( $Re_\tau \sim 7000$ ), using the Hilbert transformation in an attempt to quantify the relationship between large-scale fluctuations and any amplitude modulation of the small-scale energy in turbulent boundary layers. In particular, detailed analysis is performed on the validation and robustness of this novel procedure.

## EXPERIMENTS

The experiments were conducted in the High Reynolds Number Boundary Layer Wind-Tunnel (HRNBLWT) at the University of Melbourne with a working test section  $27 \times 2 \times 1$  m. Full details of the facility are available in Nickels *et al.* (2005). Measurements consist of boundary layer traverses using a single-normal hot-wire probe. The probe is made using a Wollaston platinum wire sensing element, operated in constant temperature mode using an AA Lab Systems AN-1003 with overheat ratio set to 1.8. The diameter  $d$  and length  $l$  of the sensing element were chosen such that the viscous scaled length  $l^+ = lU_\tau/\nu = 22$  with  $l/d = 200$ , to avoid any spatial resolution influences (Hutchins *et al.*, Under Review). The non-dimensional time interval between samples was kept in the range  $\Delta T^+ \simeq 0.4 - 0.6$  to ensure that the smallest scales were adequately resolved. A sufficiently long sample length  $T$ , in the range of 5000–14000 boundary layer turnover times ( $TU_\infty/\delta$  where  $U_\infty$  is the freestream velocity), was necessary to converge the energy contained in the largest-scales. The friction velocity  $U_\tau$  was calculated from a Clauser chart fit (using log-law constants  $\kappa = 0.41$  and  $A = 5.0$ ). Boundary layer thickness  $\delta$  is calculated from a

modified Coles law of the wake fit (Jones *et al.*, 2001). Measurements were made for this study at a Reynolds number  $Re_\tau = 7300$ .

### AMPLITUDE MODULATION

It is now well known that as the Reynolds number increases, a second distinct peak appears in the pre-multiplied energy spectra map of the streamwise velocity component (Hutchins & Marusic, 2007a). A representation of this map for the present data is given in figure 1 where the coordinate system,  $x$ ,  $y$ , and  $z$  refers to the streamwise, spanwise and wall-normal directions. The spectral density function of the streamwise velocity fluctuation is described by  $\phi_{uu}$  and the streamwise wavenumber and wavelength are denoted by  $k_x$  and  $\lambda_x$  respectively (where  $\lambda_x = 2\pi/k_x$ ). Over-bars indicate time-averaged values and the superscript “+” is used to denote viscous scaling length  $z^+ = zU_\tau/\nu$ , velocity  $u^+ = u/U_\tau$  and time  $t^+ = tU_\tau^2/\nu$ .

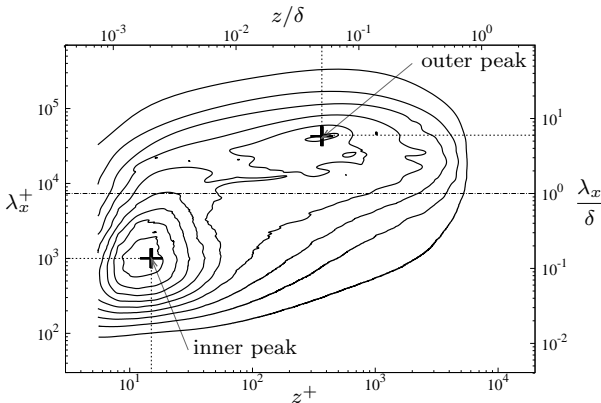


Figure 1: Iso-contours representation of the pre-multiplied energy spectra of streamwise velocity fluctuation  $k_x \phi_{uu}/U_\tau^2$  ( $Re_\tau = 7300$ ); Levels are from 0.2 to 1.8 in steps of 0.2.; The “+” symbols mark the inner ( $z^+ = 15$ ,  $\lambda_x^+ = 1000$ ) and outer peaks ( $z/\delta = 0.05$ ,  $\lambda_x/\delta = 6$ ); The horizontal dot-dashed line shows the location of the spectral filter ( $\lambda_x = \delta$ ).

In addition to the near-wall cycle peak (inner-peak), a clear peak appears in the logarithmic region (outer-peak) in figure 1. This peak was related by Hutchins & Marusic (2007a) to the superstructure type events associated with the log-region. They also noted that this large-scale energy imposes a strong signature at the wall, with low-wavenumber events superimposed on the near-wall cycle, high frequency, streamwise fluctuations. Further investigations also reveal that the large- and small-scales interaction does not appear to be only a linear process of superposition.

A more advanced study of the relationship between large- and small-scales is performed by decomposing a fluctuating velocity signal into a large- and a small-scale component (applying wavelength pass filter below and above a careful chosen cutoff wavelength). From the map in figure 1,  $\lambda_x = \delta$  appears to be a reasonable location to separate large- and small-scale components. An example of such decomposition is given in figure 2 for a sample  $u^+$  at  $z^+ = 15$ . The raw signal  $u^+$  (Fig. 2a) is decomposed in a large-  $u_L^+$  ( $\lambda_x > \delta$ ) and small-scale  $u_S^+$  ( $\lambda_x < \delta$ ) components (Fig. 2b and 2c respectively). It is observed that under the negative signature of a superstructure (large negative fluctuation excursion of the large-scale component  $u_L^+$ ) the small-scale component seems to be amplitude modulated, e.g. lower fluctuations are observed. To analyse and quantify this modulation ef-

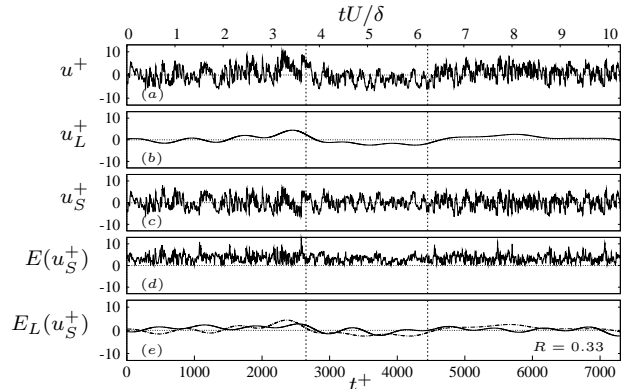


Figure 2: Example of small-scale decomposition on fluctuating  $u^+$  velocity signal in the near-wall region,  $z^+ = 15$ ; (a) raw fluctuating component  $u^+$ ; (b) large-scale fluctuation  $\lambda_x/\delta > 1$ ; (c) small-scale fluctuation  $\lambda_x/\delta < 1$ ; (d) its envelope; and (e) filtered envelope (solid line) against the large-scale component (dot-dashed). For comparison, the mean of the filtered envelope has been adjusted to zero. Dashed vertical lines show region of negative large-scale fluctuation.

fect we introduce the Hilbert transformation applied to the small-scales component  $u_S^+$ . The Hilbert transformation is well known to extract the envelope of any signal (Papoulis, 1962; Bendat & Piersol, 1986; Hahn, 1996; Bracewell, 2000; Mathis *et al.*, 2007), which in amplitude modulation processing corresponds to the modulating signal (assumed here to be the large-scale component). Hence, the correlation coefficient between the envelope of the small-scale component and the large-scale component should return a direct indicator of the level of amplitude modulation. However, the envelope returned by the Hilbert transform will track not only the large-scale modulation due to the log-region events, but also the small-scale variation in the “carrier” signal as can be seen in figure 2d. To remove this effect, we filter the envelope at the same cutoff wavelength as the large-scale signal ( $\lambda_x > \delta$ ). This returns a filtered envelope  $E_L(u_S^+)$  describing the modulation. It is now possible to compute a meaningful correlation coefficient  $R$ , of the filtered envelope  $E_L(u_S^+)$  with the large-scale velocity fluctuation  $u_L^+$

$$R = \frac{\overline{u_L^+ E_L(u_S^+)}}{\sqrt{\overline{u_L^{+2}}} \sqrt{\overline{E_L(u_S^+)^2}}} \quad (1)$$

where  $\sqrt{\overline{u^2}}$  denotes the r.m.s value of the signal  $u$ . A full description of the process to qualify the amplitude modulation level in any fluctuating velocity signal is given in figure 3. For the sample shown in figure 2e, the degree of amplitude modulation  $R$  is found to be 0.33, which is a significant correlation.

A complete evaluation of the degree of amplitude modulation across the turbulent boundary layer is obtained by applying the procedure for the streamwise fluctuating velocity component  $u^+$  at all wall-normal locations  $z^+$ . The resulting modulation coefficient,  $R(z^+)$ , is a strong function of  $z^+$  (as seen in figure 4). It appears that the viscous sub-layer of elongated high- and low-speed streaks (Kline *et al.*, 1967) resides under a strong amplitude modulation effect ( $0.2 \leq R \leq 0.7$ ) caused by low wave-number motions associated with the log-region. Away from the wall, the modulation coefficient describes a logarithmic evolution

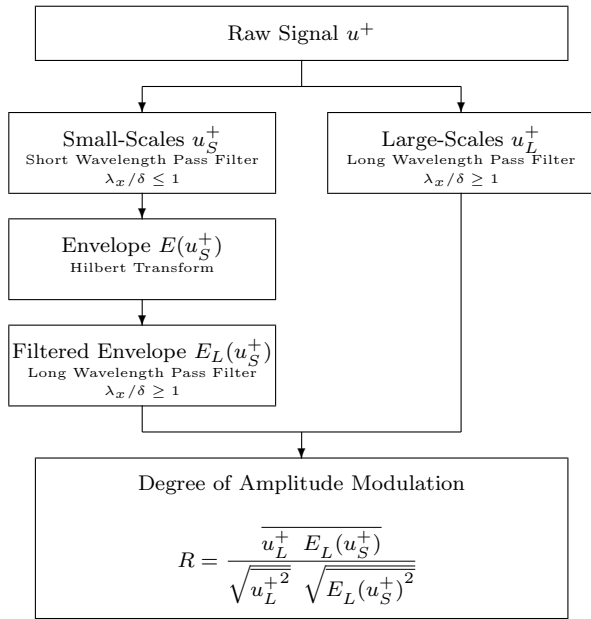


Figure 3: Procedure to determine the degree of amplitude modulation of the large-scale motions onto the small-scale events contained in any fluctuating velocity signal.

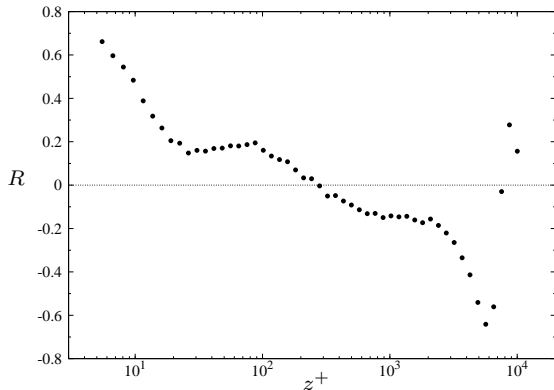


Figure 4: Wall-normal evolution of the degree of amplitude modulation  $R(z^+)$ ;  $Re_\tau = 7300$ .

decreasing progressively to reach a zero approximately at the geometric mid-point of the log layer  $z^+ \approx 300$  (on a log plot). A reversal in correlation behaviour appears beyond. This is in good agreement with to the observations of Hutchins & Marusic (2007b) who found that the small-scale energy was smaller under negative large-scale fluctuations up to the middle of the log-region, after which a reversal occurred (and the small-scale fluctuations were more energetic under negative large-scale excursions). At the top edge of the boundary layer the high negative peak in the correlation corresponds to the intermittency effect. It was observed from a cursory analysis of a velocity signal in the outer wake region that small-scale fluctuations are totally embedded in the intermittent large-scale signature.

It is noteworthy that the shape of the amplitude modulation coefficient  $R(z^+)$  appears remarkably similar to the skewness of the streamwise fluctuating velocity. Mathis *et al.* (In Press) have shown that a similar Reynolds number trend appears between the skewness (Metzger & Klewicki, 2001)

and the modulation coefficient in the buffer layer: with increasing Reynolds number the minimum of  $S(z^+)$  and  $R(z^+)$  increases from negative to positive values. However, it is difficult to understand why these two profiles should look so similar, when they refer to such different statistical quantities. The skewness is a measure of the asymmetry of the probability distribution of a signal about the mean. The modulation coefficient returns only a measure of the degree of amplitude modulation. As a final point, it is noted that both quantities are related to the phase information between large- and small-scale events.

## VALIDATION AND ROBUSTNESS

The process developed above involves numerous steps of calculation. Therefore to remove any doubt over the veracity of the results, we study here the robustness of the process. In the first instance, a synthetic signal is used to demonstrate that no artificial degree of modulation can result from the different mathematical tools. We also study the effect of the cutoff wavelength involved in the wavelength pass filters. This is performed by two ways. First, we compare the effect of the convective velocity which is used to obtain length-scale information  $\lambda_x$  from a time signal. Secondly, we analyse the dependency between the degree of modulation and the chosen cutoff wavelength. Several cutoff wavelengths are tested, located between the inner- and the outer-peaks.

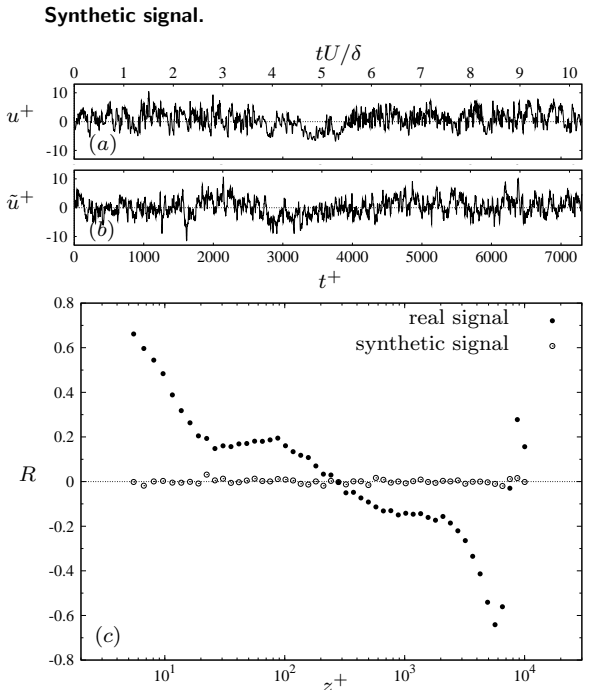


Figure 5: Comparison of the amplitude modulation procedure applied to a real signal with the procedure applied to a synthetic phase scrambled signal ( $z^+ = 15$ ,  $Re_\tau = 7300$ ); (a) instantaneous sample of a real  $u^+$  fluctuating signal; (b) instantaneous sample of a synthetic  $\tilde{u}^+$  fluctuating signal; (c) correlation coefficient  $R(z^+)$  between the large-scale component and the filtered envelope of the small-scale component.

The synthetic signal is constructed from the original velocity signal. After converting the original signal into Fourier space, the phase information (the phase of each Fourier

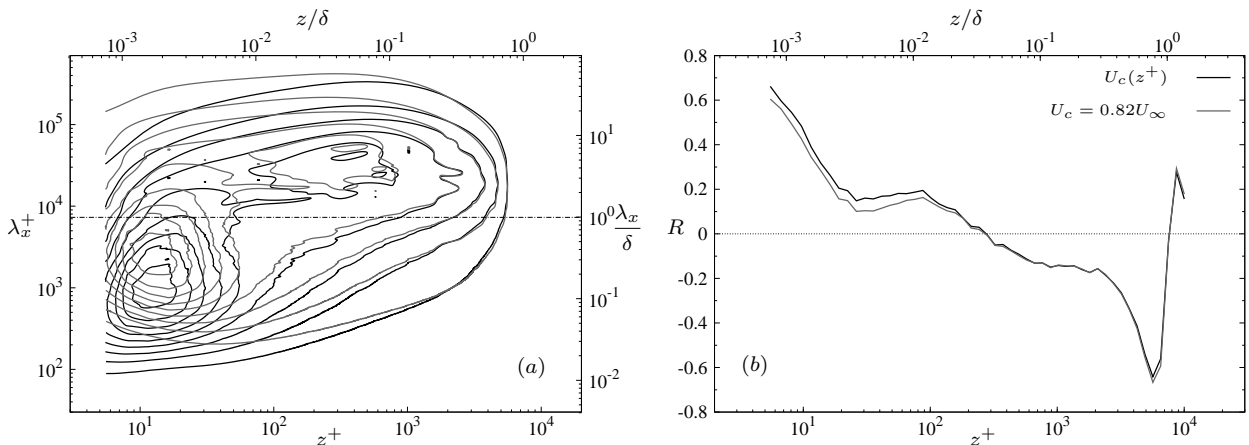


Figure 6: Effect of the convection velocity,  $Re_\tau = 7300$ ; (a) Iso-contours of the pre-multiplied energy spectra of streamwise velocity fluctuation  $k_x \phi_{uu}/U_\tau^2$ , dark lines contours show the map using local convective velocity  $U_c(z^+)$ , gray lines contours show the map using global convective velocity  $U_c = 0.82U_\infty$ , contours are from 0.2 to 1.8 in steps of 0.2. Horizontal dot-dashed lines show the location of the spectral filters ( $\lambda_x = \delta$ ). (b) Comparison of the modulation coefficient for local (dark line) and global (gray line) convection velocity.

coefficient) is scrambled by replacing it with a randomly generated number between 0 and  $2\pi$ . The amplitude is kept unchanged. An inverse Fourier transformation is applied, allowing us to obtain a synthetic signal with matched energy, but scrambled phase. A sample of each signal is shown in figures 5a and 5b for the wall-normal location  $z^+ = 15$ . Both signals look very much like turbulent fluctuating  $u^+$  velocity signals. Further analysis of the synthetic signal reveals that its energetic signature is identical to the energetic signature of the original signal. However, it is found that the synthetic signal has a zero skewness and a Gaussian distribution (kurtosis of 3) all across the boundary layer, whereas the original signal has a wall-normal dependent skewness and kurtosis. A cursory inspection of synthetic signal sample does not reveal any sign of amplitude modulation as appears in the real signal (Fig. 2). This is confirmed by calculating the degree of amplitude modulation of the synthetic signal across the boundary layer. A comparison  $R(z^+)$  between real and synthetic signals is given in figure 5c. The correlation coefficient  $R(z^+)$  for the synthetic signal exhibits a zero level across the entire boundary layer whereas for the real signal (which is reproduced from figure 4),  $R(z^+)$  returns a strong wall-normal dependency.

#### Effect of the convection velocity.

A major stage of the demodulation procedure is to decompose the initial signal into small- and large-scale components using some suitably selected wavelength pass filter. The choice of this cutoff wavelength is largely based on the pre-multiplied energy spectra map (Fig. 1). It is noteworthy that the wavelength calculated at each wall-normal location is obtained using a local convection velocity. However, the determination of the true convection velocity in turbulent boundary layers remains a controversial subject (Dennis & Nickels, 2008). Regarding it as local (where local convection velocity is determined from the local mean  $U_c(z^+) = \overline{U}(z^+)$ ), or global (where the convection velocity is given by some constant across the boundary layer e.g.  $U_c = 0.82U_\infty$ ) results in changes to the shape of the pre-multiplied energy spectra map. Both contours are compared in figure 6a, where dark lines represent contours using local

convective velocity (reproduced from Fig. 1), and gray lines show contours obtained using a global convection velocity. The buffer and log-layers are the most affected by the choice of the convective velocity, resulting in a significant change in the inner-peak location (moved from  $\lambda_x^+ = 1000$  to  $\sim 2200$ ). The outer-peak and the top edge of the boundary layer remain relatively unaffected. Consequently, with constant  $U_c$ , both inner- and outer-peaks are moved closer together. However, the cutoff wavelength ( $\lambda_x = \delta$ ) remains between these two peaks, and still seems to be a reasonable location to separate large- and small-scale motions. It is recalled that the goal of this analysis is to study the robustness of the amplitude modulation procedure, and not to become embroiled in debates surrounding appropriate choice of convection velocity. A more detailed discussion on this subject can be found in the work of Dennis & Nickels (2008). Regardless, the amplitude modulation procedure has been applied for each case, and results are plotted in figure 6b. The dark line shows the original result, and the gray line represents results obtained using the global velocity. Similar to the pre-multiplied energy spectra map, only the buffer and log-layers are affected, but weakly. The maximum discrepancy between both results is less than 5%. It appears that the demodulation procedure (Fig. 3) is somewhat robust to any error occurring in the construction of the pre-multiplied energy spectra map (due to convection velocity).

#### Effect of the cutoff wavelength.

Not only the convection velocity can affect the amplitude modulation level, but also the location of the cutoff wavelength. A careful analysis of this point is performed here where several cutoff wavelengths are studied, chosen between the inner-peak ( $\lambda_x^+ = 1000$ ) and the outer-peak ( $\lambda_x \sim 6\delta$ ) locations. It is noteworthy that the local convection velocity is used here. Four cutoff wavelengths are tested, represented by the dot-dashed lines on the pre-multiplied energy spectra map in figure 7a. For each of them, the corresponding modulation coefficient is plotted against the wall-normal position in figure 7b. The overall shape of  $R(z^+)$  appears to remain unaffected, but a discrepancy in levels is observed, mainly in the buffer layer. Considering that the set of cutoff

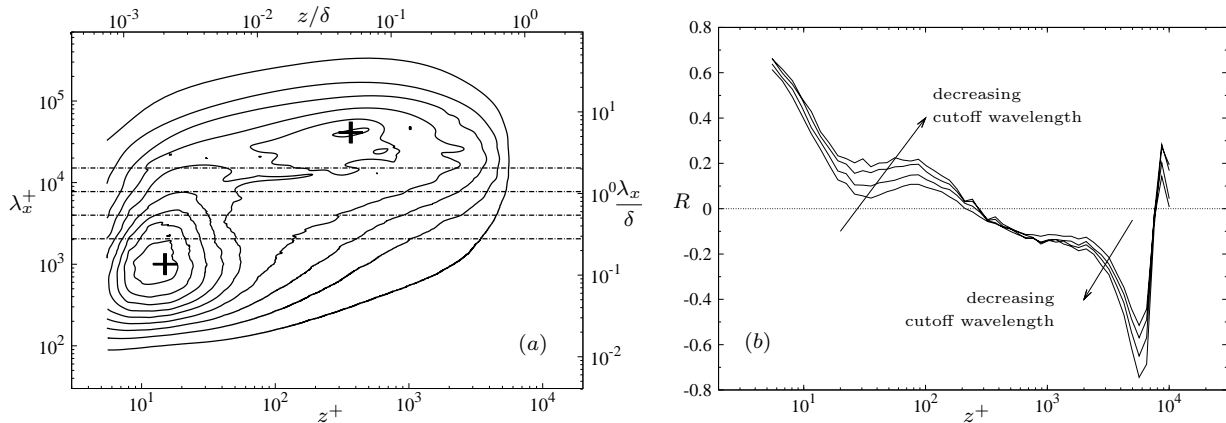


Figure 7: Effect of the cutoff wavelength; (a) Iso-contours of the pre-multiplied energy spectra of streamwise velocity fluctuation  $k_x \phi_{uu} / U_\tau^2$  with contours from 0.2 to 1.8 in steps of 0.2; Horizontal dot-dashed lines show the locations of the cutoff wavelengths; The large “+” mark the inner-peak ( $z^+ = 15$ ,  $\lambda_x^+ = 1000$ ) and the outer-peak ( $z/\delta = 0.06$ ,  $\lambda_x/\delta = 6$ ); (b) comparison of the modulation coefficients.

wavelengths covers one order of magnitude, the difference in levels noted in the buffer region appears relatively weak.

In Mathis *et al.* (In Press), a larger number of cutoff wavelengths were tested. The maximum correlation in the buffer layer actually peaks for a cutoff  $\lambda_x/\delta = 0.2$ , after which, for smaller  $\lambda_x/\delta$ , the magnitude of the correlation will reduce.

All of these results demonstrate a robustness and reliability for the procedure in assessing the degree of amplitude modulation between the large-scales and the small-scale motions.

## CONCLUSION

A novel procedure, using the Hilbert transformation applied to spectrally filtered streamwise fluctuating velocity signal, has been developed to characterise the degree of amplitude modulation taking place between large- and small-scale motions in turbulent boundary layer. Using the preliminary scale decomposition suggested by Hutchins & Marusic (2007b), it is shown that the large-scale component of any streamwise fluctuating velocity signal can be viewed as a modulating signal whilst the small-scale component is similar to a modulated signal. Consequently, the near-wall cycle resides under a strong non-linear amplitude modulation effect owing to the large-scale motions.

The amplitude modulation procedure developed through this paper constitutes a valuable tool to analyse the scale interactions in turbulent boundary layers. The veracity of the results is reinforced here by an extended study of the different parameters used in the procedure. It is shown that the estimation of the degree of amplitude modulation is highly robust to any error which might be introduced through the construction of the pre-multiplied energy spectra map, the choice of the cutoff wavelength or any artefact induced by other mathematical tools.

## ACKNOWLEDGEMENT

We gratefully acknowledge the financial support of the Australian Research Council through grants DP0663499, FF0668703, and DP0984577.

## REFERENCES

- ADRIAN, R. J., MEINHART, C. D. & TOMKINS, C. D. 2000 Vortex organization in the outer region of the turbulent boundary layer. *J. Fluid Mech.* **422**, 1–54.
- DEL ÁLAMO, J. C., JIMÉNEZ, J., ZANDONADE, P. & MOSER, R. D. 2004 Scaling of the energy spectra of turbulent channels. *J. Fluid Mech.* **500**, 135–144.
- BENDAT, J. S. & PIERSON, A. G. 1986 *Random Data: Analysis and Measurement Procedure*, 2nd edn. Wiley-Interscience Publication.
- BRACEWELL, R. 2000 *The Fourier transform and its applications*, 3rd edn. McGraw-Hill.
- DENNIS, D.J.C. & NICKELS, T.B. 2008 On the limitations of Taylor’s hypothesis in constructing long structures in a turbulent boundary layer. *J. Fluid Mech.* **614**, 197–206.
- GANAPATHISUBRAMANI, B., LONGMIRE, E. K. & MARUSIC, I. 2003 Characteristics of vortex packets in turbulent boundary layers. *J. Fluid Mech.* **478**, 35–46.
- HAHN, S. L. 1996 *The Hilbert transforms in signal processing*. Artech House.
- HOYAS, S. & JIMÉNEZ, J. 2008 Reynolds number effects on the Reynolds-stress budgets in turbulent channels. *Phys. Fluids* **20**.
- HUTCHINS, N., HAMBLETON, W. T. & MARUSIC, I. 2005 Inclined cross-stream stereo particle image velocimetry measurements in turbulent boundary layers. *J. Fluid Mech.* **541**, 21–54.
- HUTCHINS, N. & MARUSIC, I. 2007a Evidence of very long meandering features in the logarithmic region of turbulent boundary layers. *J. Fluid Mech.* **579**, 1–28.
- HUTCHINS, N. & MARUSIC, I. 2007b Large-scale influences in near-wall turbulence. *Phil. Trans. R. Soc. Lond. A* **365**, 647–664.
- HUTCHINS, N., NICKELS, T., MARUSIC, I. & CHONG, M. S. Under Review Spatial resolution issues in hot-wire anemometry. *J. Fluid Mech.*
- JIMÉNEZ, J. & PINELLI, A. 1999 The autonomous cycle of near-wall turbulence. *J. Fluid Mech.* **389**, 335–359.
- JONES, M. B., MARUSIC, I. & PERRY, A. E. 2001 Evolution and structure of sink-flow turbulent boundary layers. *J. Fluid Mech.* **428**, 1–27.
- KIM, K. C. & ADRIAN, R. J. 1999 Very large-scale motion in the outer layer. *Phys. Fluids* **11**, 417–422.

- KLINE, S. J., REYNOLDS, W. C., SCHRAUB, F. A. & RUNDSTADLER, P. W. 1967 The structure of turbulent boundary layers. *J. Fluid Mech.* **30**, 741–773.
- MATHIS, R., HUTCHINS, N. & MARUSIC, I. 2007 Evidence of large-scale amplitude modulation on the near-wall turbulence. In *16th Australasian Fluid Mech. Conf.*. Gold Cost, Australia.
- MATHIS, R., HUTCHINS, N. & MARUSIC, I. In Press Large-scale amplitude modulation of the small-scale structures in turbulent boundary layers. *J. Fluid Mech.* .
- METZGER, M. M. & KLEWICKI, J. C. 2001 A comparative study of near-wall turbulence in high and low Reynolds number boundary layers. *Phys. Fluids* **13**, 692–701.
- NICKELS, T. B., MARUSIC, I., HAFEZ, S. & CHONG, M. S. 2005 Evidence of the  $k_1^{-1}$  law in high-Reynolds number turbulent boundary layer. *Phys. Rev. Lett.* **95**, 074501.
- PANTON, R. L. 2001 Overview of the self-sustaining mechanisms of wall turbulence. *Prog. Aerosp. Sci.* **37**, 341–383.
- PAPOULIS, A. 1962 *The Fourier integral and its applications*. McGraw-Hill.